

C-Terminal Titin Deletions Cause a Novel Early-Onset Myopathy with Fatal Cardiomyopathy

Virginie Carmignac, MS,^{1,2} Mustafa A. M. Salih, MD,³ Susana Quijano-Roy, MD, PhD,^{1,2,4} Sylvie Marchand, PhD,⁵ Molham M. Al Rayess, MD, FCAP,⁶ Maowia M. Mukhtar, PhD,⁷ Jon A. Urtizberea, MD,⁸ Siegfried Labeit, MD,⁹ Pascale Guicheney, PhD,^{1,2} France Leturcq, PhD,¹⁰ Mathias Gautel, MD, PhD,¹¹ Michel Fardeau, MD, PhD,^{1,2} Kevin P. Campbell, PhD,¹² Isabelle Richard, PhD,⁵ Brigitte Estournet, MD,⁴ and Ana Ferreiro, MD, PhD^{1,2}

Objective: The giant protein titin is essential for striated muscle development, structure, and elasticity. All titin mutations reported to date cause late-onset, dominant disorders involving either skeletal muscle or the heart. Our aim was to delineate the phenotype and determine the genetic defects in two consanguineous families with an early-onset, recessive muscle and cardiac disorder.

Methods: Clinical and myopathological reevaluation of the five affected children, positional cloning, immunofluorescence, and Western blot studies were performed.

Results: All children presented with congenital muscle weakness and childhood-onset fatal dilated cardiomyopathy. Skeletal muscle biopsies showed minicores, centrally located nuclei, and/or dystrophic lesions. In each family, we identified a homozygous titin deletion in exons encoding the C-terminal M-line region. Both deletions cause a frameshift downstream of the titin kinase domain and protein truncation. Immunofluorescence confirmed that truncated titins lacking the C-terminal end were incorporated into sarcomeres. Calpain 3 was secondarily depleted.

Interpretation: M-line titin homozygous truncations cause the first congenital and purely recessive titinopathy, and the first to involve both cardiac and skeletal muscle. These results expand the spectrum of early-onset myopathies and suggest that titin segments downstream of the kinase domain are dispensable for skeletal and cardiac muscle development, but are crucial for maintaining sarcomere integrity.

Ann Neurol 2007;61:340–351

Early-onset myopathies are inherited muscle disorders that manifest typically from birth or infancy with hypotonia, muscle weakness, and delayed motor development. From clinical features and particularly muscle biopsy findings, two main categories of early-onset myopathies have been established. The congenital myopathies (CMs) are characterized by particular changes in the muscle fiber structure, without fiber necrosis, regeneration, or significant endomysial fibrosis.¹ These latter myopathological features are referred to as “dys-

trophic signs” and, when coexisting with infantile weakness, define a different nosological group, the congenital muscular dystrophies (CMDs).² CMDs and CMs are genetically heterogeneous. Most of the 12 genes identified in CMD encode proteins that form the extracellular matrix or are involved in glycosylation.² Five of the nine genes associated with CMs^{3,4} encode proteins that are essential for the structure and contractility of the sarcomere, the basic functional unit of striated muscles.

From the ¹Institut National de la Santé et de la Recherche Médicale U582, Institut de Myologie, Groupe Hospitalier Pitié-Salpêtrière; ²Université Pierre et Marie Curie, Paris, France; ³Division of Pediatric Neurology, Department of Pediatrics, College of Medicine, Riyadh, Saudi Arabia; ⁴Service de Pédiatrie-Réanimation Infantile, Hôpital Raymond Poincaré, Garches, France; ⁵Génethon, Centre National de la Recherche Scientifique, Unité Mixte de Recherche, 8115, Evry, France; ⁶Department of Pathology, College of Medicine, Riyadh, Saudi Arabia; ⁷Institute of Endemic Diseases, University of Khartoum, Khartoum, Sudan; ⁸Hôpital Marin, Hendaye, France; ⁹Institute for Anaesthesiology and Intensive Care, University Clinic Mannheim, Mannheim, Germany; ¹⁰Laboratoire de Biologie Génétique, Hôpital Cochin, Paris, France; ¹¹Muscle Signaling and Development, The Randall Division of Cell and Molecular Biophysics and the Cardiovascular Division, New Hunt's House,

King's College London, London, United Kingdom; and ¹²Howard Hughes Medical Institute, Department of Physiology and Biophysics, Internal Medicine, and Neurology, University of Iowa Roy J. and Lucille A. Carver College of Medicine, Iowa City, IA.

Received Nov 10, 2007, and in revised form Dec 21. Accepted for publication Jan 5, 2007.

Published online Apr 24, 2007, in Wiley InterScience (www.interscience.wiley.com). DOI: 10.1002/ana.21089

Address correspondence to Dr Ferreiro, INSERM U582, Institut de Myologie, Groupe Hospitalier Pitié-Salpêtrière, 47 Boulevard de l'Hôpital, 75651 Paris, France.
E-mail: a.ferreiro@myologie.chups.jussieu.fr

Conversely, mutations in sarcomere proteins have also been associated with the so-called late-onset myopathies, which manifest generally from the fourth to fifth decade of life. This is particularly the case for the giant protein titin, one of the major sarcomere components, which is considered to play a crucial role in striated muscle development, structure, elasticity, and cell signaling (OMIM 188840). Titin, encoded by the 363-exon titin gene (*TTN*), is the largest protein known (up to 4,200kDa).⁵ Each titin molecule spans half of the sarcomere (>1 μm), connecting the Z-disk (amino terminus) with the M-line (carboxy terminus).⁵ The 13 *TTN* mutations currently reported manifest in the heterozygous state as late-onset, autosomal dominant disorders involving either heart or skeletal muscle. Heterozygous missense (7) or nonsense (2) mutations in the N-terminal third of titin have been associated with hypertrophic^{6,7} or dilated cardiomyopathy.⁷⁻⁹ In contrast, four mutations changing amino acid residues in M-line titin lead to the three skeletal muscle titinopathies yet described: (1) late-onset autosomal dominant myopathy with proximal weakness and early respiratory muscle involvement¹⁰; (2) tibial muscular dystrophy (TMD; MIM 600334)^{11,12}; or (3) limb-girdle muscular dystrophy type 2J (LGMD2J).^{11,13} TMD is a distal myopathy presenting in the fourth to seventh decade of life. The most common mutation in TMD patients (FINmaj, in exon Mex6) changes four amino acids near the C-terminal end of titin without protein truncation.¹¹ Noticeably, four patients from TMD families were homozygous for the FINmaj mutation and presented from the end of the first to the third decades with the more severe LGMD2J (MIM 608807).¹¹ Although the LGMD2J phenotype was tentatively classified as recessive, these rare cases are best understood as the homozygous manifestation of a dominant mutation, which in the heterozygous parents manifests with full penetrance as TMD¹¹ (MIM 608807).

Although the exons affected by the reported *TTN* mutations are generally expressed in skeletal and cardiac titin isoforms, no phenotype involving both skeletal muscle and heart has been identified. In mice, early deletion of M-line titin exons 358 and 359, encompassing the serine/threonine kinase domain encoded by exon 358, leads to embryonic lethality.¹⁴ In humans, homozygous defects leading to absence of a titin portion have never been reported, and it has been generally considered that major homozygous titin defects would not be compatible with life.¹⁵ Furthermore, no congenital or purely recessive titinopathy has been described.

We report here a novel titinopathy that, in contrast with the previously described examples, involves both heart and skeletal muscle, has a congenital onset, and is purely recessive. We describe the distinct phenotype

identified in two consanguineous families initially diagnosed with CM and CMD, respectively. Furthermore, we demonstrate that this phenotype is due to homozygous out-of-frame *TTN* deletions, which lead to a total absence of titin's C-terminal end from striated muscles and to secondary calpain 3 depletion. These results establish that homozygous truncations of M-line titin preserving the kinase domain are compatible with life but cause a novel, severe disorder, thereby expanding the spectrum of early-onset myopathies.

Subjects and Methods

Patients

This study included five patients (P1 to P5) from two families (F1 and F2) of Moroccan and Sudanese origin, respectively. Inclusion criteria were: (1) congenital muscle weakness, (2) childhood-onset dilated cardiomyopathy, (3) both dystrophic and minicore-like morphological lesions, and (4) normal immunolabeling of the proteins previously associated with early-onset myopathies. Both parental couples were consanguineous and healthy. Phenotypical findings in F2 have been partially reported elsewhere.^{16,17}

The clinical phenotype of all patients was evaluated retrospectively according to clinical pictures and records. Unaffected family members were specifically examined for this study, including muscle magnetic resonance imaging (MRI), except for the parents in F1 who declined this complementary evaluation. Muscle samples, blood samples, DNA, and muscle MRIs were obtained after informed consent in agreement with local ethic committees.

Morphological Studies

At least one skeletal muscle biopsy was obtained from each patient (total = 7). Heart muscle samples were taken from P2 (endomyocardial biopsy and postmortem sample) and P3 (after heart explant for transplantation).

All samples were frozen and processed for standard histological and histochemical stainings. In addition, three muscle samples from P2, P4, and P5 were fixed and processed for electron microscopy.¹⁸

Standard indirect immunohistochemical studies were performed on skeletal muscle transverse cryosections from P3, P4, and P5, using antibodies against dystrophin, α-, β-, γ-, and δ-sarcoglycans, β-dystroglycan, integrin α7 and laminin α2 chain, as described elsewhere,¹⁶ as well as α-dystroglycan (1/100; Euromedex, Souffelweyersheim, France). Skeletal muscle from P3 was also labeled with antibodies against emerin (NCL-emerin, 1/40; Novocastra, Newcastle, United Kingdom) and desmin (1/100; Dako, Carpinteria, CA). Furthermore, titin truncation was verified on skeletal (P3, P4) and heart (P2) muscle using the following epitope-specific antibodies: monoclonal anti-titin T51 (1/50),¹⁹ polyclonal anti-titin A168-170 (1/100),¹¹ and monoclonal NCL-titin (1/100; Novocastra). Sections were incubated for 2 hours at room temperature with primary antibodies, followed by polyclonal rabbit anti-mouse immunoglobulin/fluorescein isothiocyanate (Ig/FITC, 1/300; Dako) or Alexa 488 goat anti-rabbit (1/500; Molecular Probes, Leiden, the Netherlands). Immunofluorescence was visualized with an Axio-

phot2 fluorescence microscope (Zeiss, Oberkochen, Germany) and acquired with a Photometrics Cool Snap fx camera (Roper Scientific, Tucson, AZ).

Genetic Analysis

We used standard procedures to extract genomic DNA from frozen muscle biopsies (for deceased P4 and P5), blood samples, or lymphoblastoid cell lines.

GENOTYPING. A whole-genome screening was performed for F1 using 330 fluorescently labeled polymorphic microsatellites with an average spacing of 10 to 25cM (Applied Biosystems, Warrington, United Kingdom).²⁰ Twenty-seven additional markers were amplified for fine mapping of potential loci. Besides, we excluded linkage to three genes previously implicated in familial cardiomyopathy with skeletal muscle involvement, using microsatellites flanking *FKRP* (fukutin-related protein gene),²¹ *LMNA* (lamin A/C gene),²² and *MYH7* (β -myosin heavy chain gene).²³ Results were analyzed by the Genotyper 2.0 software (Applied Biosystems).

LINKAGE ANALYSIS. Linkage analysis was performed using the easyLINKAGE package,²⁴ under the assumptions of autosomal recessive inheritance, an equal recombination frequency for female and male subjects, a disease gene frequency of 0.0001, one liability class, and a penetrance of 0.98. LOD scores were calculated using the SuperLink program.

TTN SEQUENCING. All titin M-band exons (Mex1-6, or 358-363) were amplified as described elsewhere,²⁵ sequenced on an ABI prism 377 automated sequencer using the BigDye terminator kit (Applied Biosystems), and analyzed using the Sequence Analysis software (Applied Biosystems).

Western Blot

Protein extraction from P3 skeletal muscle was performed from 10 transverse cryosections (20 μ m in thickness). Western blots were labeled with a cocktail of antibodies directed against dystrophin DYS1 (Dy4/6D3 rod domain; Novocastra), α -sarcoglycan (Ad1/20A6; Novocastra), and calpain 3, including Calp3d/2C4 (against exon 1– and 3–encoded domains) and Calp3c/12A2 (against exon 3– and 8–encoded domains; Novocastra), as described previously.²⁶

Results

Clinical Phenotype

We initially evaluated three male siblings (P1 to P3) born from Moroccan first-degree consanguineous parents (F1). Pregnancy, birth, and the neonatal period always were uneventful, without neonatal hypotonia. However, the three children showed delayed motor milestones during the first year of life, acquiring autonomous gait between 20 and 24 months. Clinical examination in infancy and early childhood demonstrated symmetric, generalized muscle weakness that involved predominantly lower limbs, both proximal and distal. Weakness was greatest in psoas, gluteus maximus, tib-

ialis anterior, and peroneus muscles, with relative preservation of the quadriceps. Proximal upper limbs, neck and trunk flexors, and facial muscles were also affected. Ptosis, sometimes asymmetric, was a constant finding. Remarkably, poor muscle bulk in upper limbs contrasted with relative pseudohypertrophy in lower limbs, particularly in thighs and calves (Fig 1). During the first decade of life, spinal rigidity and moderate joint and neck contractures appeared, but global motor performances were stable or tended to improve; difficulties for climbing stairs, running, and rising up from the sitting position remained the main manifestations of skeletal muscle involvement. In contrast, a dramatically progressive dilated cardiomyopathy developed in all the patients from the ages of 5 to 12 years, simultaneously with rhythm disturbances (Table). Echocardiographies demonstrated left ventricle reduced function, dilatation, and global hypokinesia, without wall hypertrophy or other anatomic abnormalities. At later stages, dilatation of the left atrium and ventricle was observed. Despite pharmacological treatment, heart failure associated with ventricular or supraventricular arrhythmias led to sudden death of the two eldest siblings at 8 and 17 years of age (see the Table). P3 had heart transplantation at 15 years, with good results, but died 2 years later because of postoperative complications after spinal fusion.

In a second first-degree consanguineous Sudanese family, two siblings (P4 and P5) presented with neonatal hypotonia and delayed motor development, acquiring independent gait at 26 months and 4 years, respectively. Both always had significant difficulties in running and climbing stairs. On examination, the main clinical findings were virtually identical to those in F1 (see Fig 1), including generalized muscle weakness that involved also the facial muscles, asymmetric ptosis (congenital in P5), and relative calf hypertrophy. After motor improvement in the first decade, dilated cardiomyopathy developed concurrently with major rhythm disturbances, namely, ventricular hyperexcitability (see the Table).^{16,17} Contractile dysfunction and dilation, initially restricted to the left ventricle, affected subsequently all chambers leading to congestive heart failure in P4. Sudden death occurred in both siblings at 19.5 and 17.5 years.

In both families, the patients who survived into the second decade showed slow progression of muscle weakness, although all remained ambulant, with or without support. Scoliosis developed only in P3 after 11 years. Cognitive functions, brain MRI, electroencephalogram, and/or evoked potentials were normal. Serum creatine kinase levels were marginally to moderately increased (1.5- to 7-fold), and electromyogram was myopathic. Respiratory function examinations in F1 showed a moderate restrictive pattern (forced vital

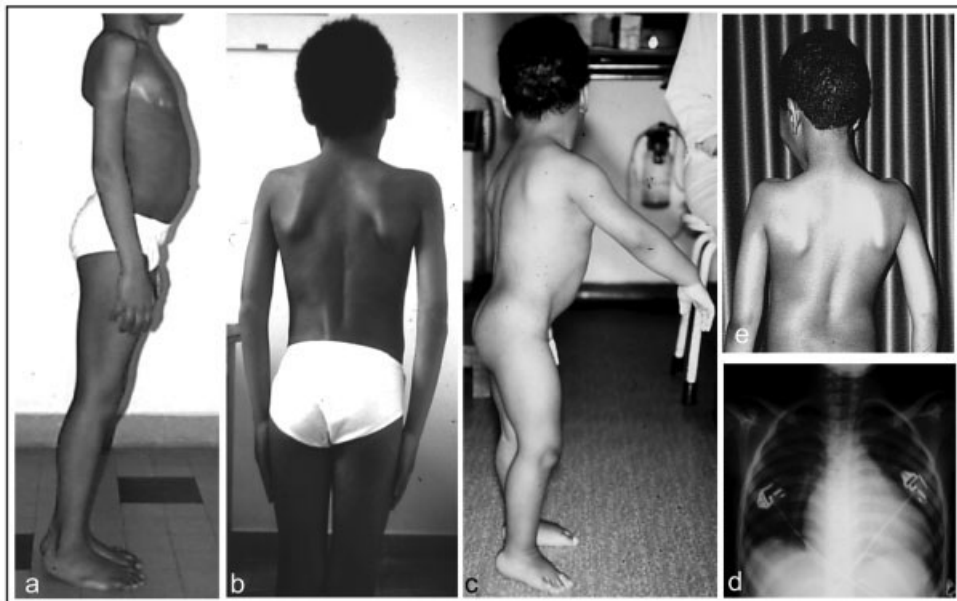


Fig 1. Common clinical phenotype in patients from Families 1 (F1; a–d) and 2 (F2; e). Lower limbs were relatively pseudohypertrophic, with bulky thighs and calves (a, c), which contrasted with the poor bulk of proximal upper limbs and thoracic muscles (a, b, e). Patient 4 (P4) showed clear deltoid amyotrophy (e). Moderate contractures were present in Achilles tendons, hips, elbows, pectoral muscles, and sternocleidomastoides (a). Progressive left ventricular dilated cardiomyopathy developed from childhood (P2 at 5 years; d). P1 (a, b); P2 (c, d); P4 (e).

capacity, 63–76%) without clinical symptoms; no patient had significant diaphragm weakness.

F1 and F2 parents, currently aged 46 to 59 years, are healthy and show no symptoms or signs of heart

or skeletal muscle dysfunction. Muscle MRI of F2 parents at 44 and 55 years was normal, including tibial muscles. In F1, a female child died in the first week of life of a congenital heart defect, allegedly a

Table. Cardiac Involvement in Families 1 (Patients 1-3) and 2 (Patients 4 and 5)

Characteristics	Patient No.				
	P1	P2	P3	P4	P5
Age at onset, yr	12	5	11	16	>12
Rhythm disturbances	Polymorphic PVC VT Sudden death	AVNRT Sudden death	PAC	Polymorphic PVC, bigeminism and trigeminism, couplets, triplets AVB Sudden death	Sudden death
SF or EF	LVSF 16% at 12 yr	LVSF 5% at 8 yr	LVSF 5% at 15 yr	LVEF 12% and RVEF 14% at 19 yr	NA
Evolution/complications	Cardioembolic stroke and hemiparesis at 14 yr	Episode of cardiogenic shock at 8 yr	Heart transplantation at 15 yr	Congestive heart failure	NA
Age at death, yr	17	8	17	19.5	17.5

Dilated cardiomyopathy developed from childhood and was dramatically progressive, leading to death between 3 and 5 years after its diagnosis. Before onset of dilated cardiomyopathy, heart function and morphology were normal as demonstrated by cardiac echographies and Holter electrocardiograph in P1 (at 3 and 11 years) and P5 (at 12 years), except for isolated left anterior fascicular block, which was present in P4 and P5 from 4 and 9 years, respectively. In both families, left ventricle hypokinesia was more marked in the septum.^{18,19} PVC = premature ventricular complexes; VT = ventricular tachycardia; AVNRT = auriculoventricular nodal reentrant tachycardia; PAC = premature atrial complexes; AVB = auriculoventricular heart block (first degree); SF = shortening fraction; EF = ejection fraction; LVSF = left ventricular shortening fraction; LVEF = left ventricular ejection fraction; RVEF = right ventricular ejection fraction; NA = not available.

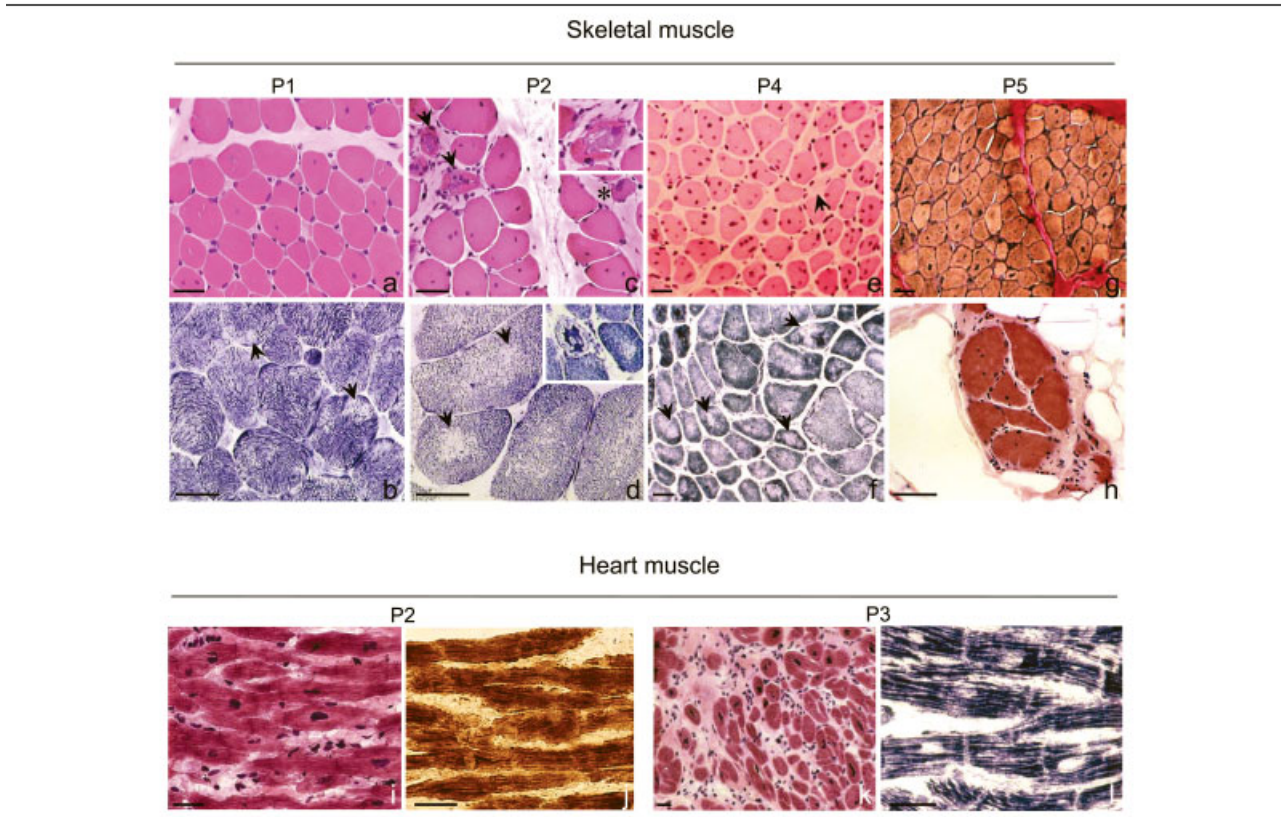


Fig 2. Skeletal and heart muscle histopathological pattern. (a–h) Skeletal muscle samples taken from Patient 1 (P1) at 3 years (deltoid; a, b), P2 at 6 years (deltoid; c, d), P4 at 14 years (quadriceps; e, f), and P5 quadriceps at 4 (g) and 10 years (h). Fiber size variability, poorly delimited oxidative-negative areas (b, d, f, arrows), and type 1 fiber uniformity were constant findings. All samples showed also a variable number of centrally located nuclei, ranging from moderate (approximately equal to 10% fibers, a) to huge (e), which tended to be more patent in the eldest and/or most severe cases. Moderate endomysial fibrosis and some sparse necrotic (arrow, e) or regenerating (asterisk, c) fibers were observed in two of the biopsies (c, e). Noticeably, these samples showed also a few small fibers with central star-shaped areas that were basophilic on hematoxylin and eosin staining (HE), dark blue with oxidative stainings, and were often rimmed by one or more centrally located nuclei (CLNs; arrow in c; boxed in c, d). The two biopsies from P5 (g, h), taken from the same muscle at 6-year interval, demonstrated severe progression of the disease, with massive muscle fiber loss associated with connective and fatty tissue infiltration in the second sample (h). (i–l) Heart muscle samples showed a dilated cardiomyopathy pattern, marked by increased interstitial fibrosis (i, k); oxidative staining was normal and myocyte disarray was notably absent (j, l), contrary to what is classically observed in hypertrophic cardiomyopathy. (i–j) P2 at 8 years; (k, l) P3 at 15 years. Longitudinal (i, j, l) and transverse cryostat sections of skeletal muscle (a–h) and myocardium (i–l); HE (a, c, e, h, i, k), NADH-TR (b, d, f, l), Van Gieson's stain (g), COX (j). Bar = 40 μ m.

ventricular malformation, on which no precise information is available. Clinical examination of the eldest 30-year-old son was normal. No other family member is reported to have a heart or muscle disorder, including the 18 total adult siblings of both F1 parents.

Morphological and Immunohistochemical Pattern

Skeletal muscle biopsies demonstrated in all patients a similar, distinct, and recognizable morphological phenotype. In early childhood, this pattern was compatible with a CM, marked by minicore-like lesions and abundant centrally located nuclei (CLNs). Dystrophic lesions of variable severity were more conspicuous in the second decade (Fig 2).

The three muscle samples taken from P1, P4, and P5 between the ages of 3 and 4 years (see Figs 2A, B, G) showed abundant minicores (foci of mitochondria depletion and sarcomere disorganization), as well as CLNs in 10 (P1) to 33% (P5) of the fibers. These structural changes coexisted with type 1 fiber predominance, increased fiber size variability, and scattered rounded, small fibers. No endomysial fibrosis or necrosis/regeneration lesions were present.

Conversely, the muscle biopsies taken at 6 and 14 years from P2 and P4, respectively, showed significant endomysial fibrosis and sparse regenerating fibers, in addition to minicores and CLNs (see Figs 2C–F). In P4's second biopsy, virtually all fibers were speckled with a myriad of relatively large CLNs (up to seven per

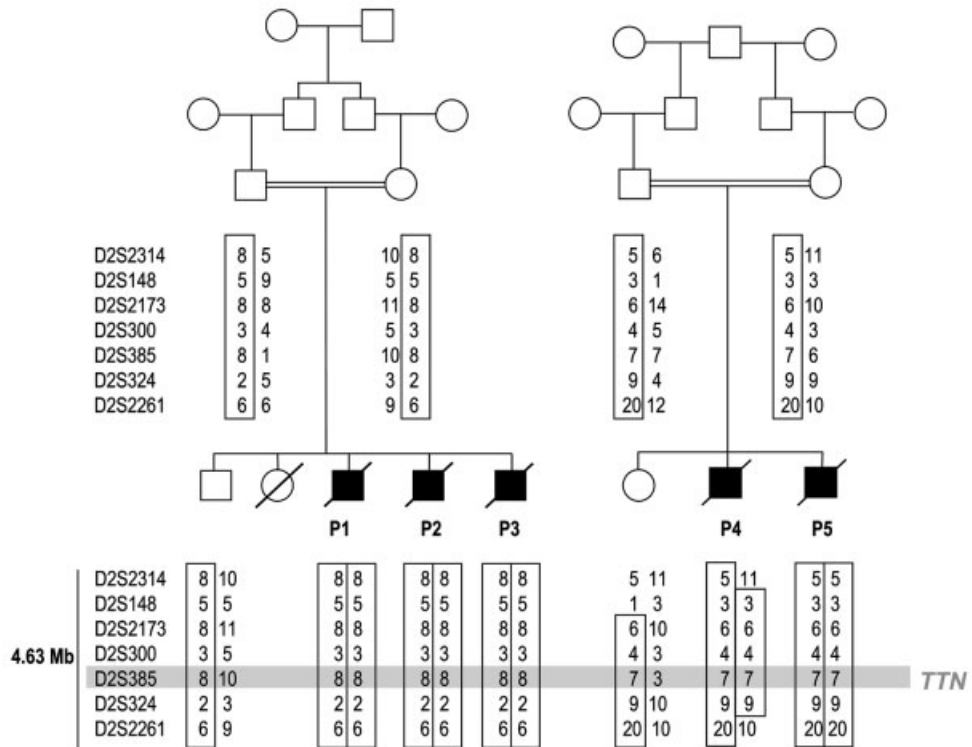


Fig 3. Pedigrees and haplotype analysis at 2q31.1-q31.3. The homozygosity region shared by both families spans 4.63 Mb and includes TTN intragenic marker D2S385 (shadowed). The locus was limited by markers D2S2314 and D2S2261, with the highest cumulative LOD score for D2S300 (LS = 3.29; $\theta = 0.00$). No common haplotype suggesting a founder effect was observed. Affected individuals are denoted by filled symbols; deceased individuals denoted by a diagonal. Consanguinity links are represented in a simplified way. For compactness, only the most relevant markers are shown. Haplotypes/markers that are homozygous in the affected individuals are boxed. Noticeably, the unaffected siblings from the two families have inherited one at-risk haplotype. The parents in Family 1 (F1) are currently 59 and 54 years old, those in F2 are 46 and 57 years old.

fiber transversal section); fibrosis was more prominent than necrosis/regeneration. In contrast, the second quadriceps biopsy from his brother P5, taken at 10 years, demonstrated massive muscle fiber loss (see Fig 2H). A paravertebral muscle sample from 15 year-old P3 showed also dystrophic features and abundant rimmed vacuoles.

Skeletal muscle ultrastructural studies in P2 and P4 confirmed the presence of multiple foci of sarcomere disruption and mitochondria depletion. These minicores spanned generally three to six contiguous sarcomeres along the longitudinal fiber axis (Fig 4), but were sometimes larger. Noticeably, some M-lines looked to be pulled apart and contrasted with comparatively preserved Z-lines, contrary to the typical minicores in which Z-line streaming is often more apparent than disintegration of the sarcomere center.¹⁸ Aside from these minicore-like lesions, the muscle fiber and sarcomere ultrastructure were normal.

Left ventricle cryosections from P2 and P3 showed marked disruption of myocardial architecture, nuclear hypertrophy, and severe endomyocardial fibrosis (see Figs 2I-L), without focal oxidative defects or significant dis-

array of the cardiomyocyte structure on light microscopy.

Immunohistochemical studies on skeletal muscle from P3, P4, and P5 showed normal expression and distribution of laminin $\alpha 2$ chain, integrin $\alpha 7$, α - and β -dystroglycan, α -, β -, γ - and δ -sarcoglycans, and dystrophin; normality of desmin and emerin was also verified in P3.

Identification of a Recessive Linkage to 2q31.1-q31.3

In the most informative family (F1), a whole-genome screen, performed to search for a new locus, allowed excluding linkage to chromosome X and to most of the genes previously implicated in dilated cardiomyopathy with skeletal muscle involvement. Flanking markers excluded more specifically three candidate genes: *FKRP*,²¹ *LMNA*,²² and *MYH7*.²³

Further analysis of the genome-wide screen results and of additional markers disclosed in all the affected members of F1 two potential regions of homozygosity by descent, in chromosomes 2 (23cM) and 3 (11.4cM). Both regions generated positive LOD scores,

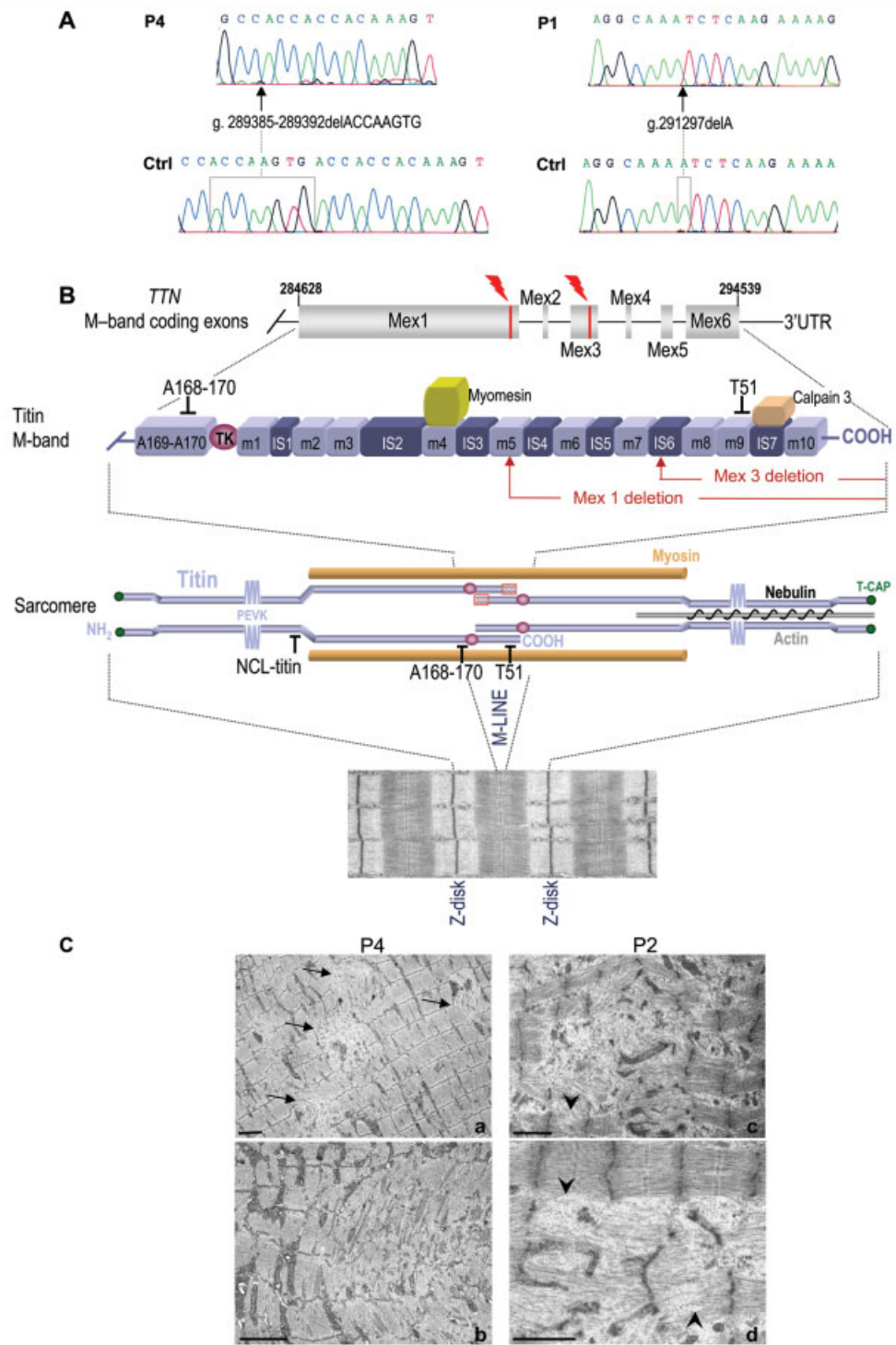


Fig 4. (A) Sequence analysis and TTN deletions on exons 358 (left) and 360 (right); Patients 4 (P4) and 1 (P1), respectively. The deleted bases are boxed in the control sequences. (B) Schematic representation of the 250kDa carboxyl-terminal M-band titin and location of the deletions; encoding exons (top), protein domains and main partners (middle), and arrangement within a normal sarcomere (bottom). Titin deletions are represented as red bars (top) or boxes (bottom). Location of the epitopes used to generate the anti-titin antibodies studied is symbolized (black marks). TK = titin kinase. (C) Ultrastructural lesions in skeletal muscle. Longitudinal electron microscope sections of biopsies from P4 (a, b) and P2 (c, d). Normal sarcomeres with preserved M-line bridges coexist with focal areas of severe myofibrillar disorganization (arrow in a); in most of them, the disrupted sarcomeres look pulled apart, curving away the contiguous ones (b, c). Some of the sarcomeres show disintegration of the M-line, which contrasts with relative preservation of the flanking Z-lines, particularly in P2 (d, arrowheads). Bar = 2.5 μm.

equivalent to the maximum F1 simulated LOD score (2.28 at $\theta = 0.00$).

To determine the actual locus and reduce its size, we obtained DNA samples from the phenotypically identical F2, and genotyped them with markers from the regions of interest. This excluded chromosome 3 and confirmed homozygous linkage to a 4.63Mb region in 2q31.1-q31.3 for both families (see Fig 3). This locus contained 68 positional candidate genes and EST, including *TTN* (2q31.2).

Identification of Homozygous TTN Deletions

Because of its selective expression in striated muscles and its implication in heart or muscular conditions, *TTN* was both a strong functional and positional candidate gene. Nevertheless, screen of this huge gene is challenging. We chose to start *TTN* mutation screen from the last M-line-encoding exons for the following reasons: (1) some of the ultrastructural lesions in our patients showed M-band but not Z-disk disruption, suggesting a preferential or earlier involvement of the sarcomere center; and (2) the previously identified *TTN* mutations associated with a skeletal muscle phenotype localize in exons 358 and 363.

Sequencing of the 6 M-band-encoding *TTN* exons (Mex1-6, or 358-363) demonstrated two different out-of-frame deletions (see Fig 4). In F1, the affected patients were homozygous for a one-base deletion on exon 360 (Mex3; g.291297delA). This mutation changes 21 amino acids and generates a stop codon that predicts truncation of titin's most C-terminal 447 amino acids (Fig 5). In F2, we identified an 8bp deletion near the 3' end of exon 358 (Mex1; g.289385-289392delACCAAGTG); a premature stop codon occurs after the addition of 8 novel amino acids, predicting a loss of the last 808 C-terminal residues, downstream the kinase domain.

Each deletion was homozygous in the patients and heterozygous in the unaffected parents and siblings. None of these nucleotide or amino acid changes has been previously reported. The affected titin segments are highly conserved in mammals and chicken. Exon Mex5 can be alternatively spliced²⁷; the other M-line exons are constitutively expressed both in skeletal and in heart muscles.

Consequences of the Mutations at the Protein Level:

Titin Truncation and Calpain 3 Depletion

To investigate the presence of truncated titin and its potential integration in the sarcomeres, we performed immunohistochemical analyses on muscles from patients P2, P3, and P4, using three epitope-specific antibodies directed against I-band or M-line titin (see Fig 5).

Skeletal and heart muscles from Mex1- and Mex3-mutated patients demonstrated a complete loss of im-

munolabeling with T51, directed against the titin m8-m9 domain encoded by the Mex3/Mex4 exons (downstream of both deletions) (see Fig 4). In contrast, all samples showed normal sarcomeric labeling with NCL-titin and A168-170, which recognize epitopes localized upstream the Mex1 deletion (the I-band subregion and a Mex1-encoded epitope immediately upstream the kinase domain, respectively). Labeling intensity and distribution with these two antibodies was comparable with that in control skeletal muscle and followed a normal cross-striated pattern on longitudinal myocardial sections. These results suggest total loss of the carboxy-terminal titin epitopes located downstream of both deletions (at least after the domain m8) and the presence of a truncated titin that appears normally integrated into the sarcomeres.

The fragment deleted in both families contains one of the two titin binding sites for calpain 3 (CAPN3), located respectively in the N2A I-band region and in the Mex5-encoded Is7 domain. Western blot on skeletal muscle from P3, homozygous for the Mex3 deletion, showed a total absence of CAPN3 (see Fig 5), demonstrating that titin truncation affects the amount of this skeletal muscle-specific protease.

Discussion

Recent progress in understanding titin function and structural organization has shown it as a unique protein, not only because of its massive size, but also because its complexity and multiple roles make it a key player in the striated muscle sarcomeres. Titin is believed to organize sarcomere assembly during myogenesis,^{28,29} to provide a scaffold for thick and thin filaments,³⁰ to account for sarcomere passive tension³¹ and elasticity,³² and to mediate cell responses via its many protein partners and interacting signaling molecules.¹⁰ Yet, the primary structural function of titin is connecting longitudinally the two transverse sarcomere scaffold structures, the Z-disc and the M-line, anchoring to both through its N- and C-terminus, respectively. Therefore, total absence of a significant portion of titin, particularly in its anchoring regions, was expected to be lethal.^{14,15} As a result of phenotype and positional cloning studies of two consanguineous families, we identified two homozygous deletions in M-line titin (Mex1 and Mex3 exons), which preserve the kinase domain but result in truncation of titin in skeletal and heart muscles. For the first time, these results provide evidence that absence of the titin domains encoded by the last five or three exons is compatible with life, but causes a severe congenital disorder.

The distinct clinical, morphological, and inheritance patterns demonstrate that these families are affected by a novel early-onset myopathy, which constitutes the first purely recessive titinopathy, the first congenital one, and also the first one involving heart and skeletal

A

Mex 1 deletion: g.289385_289392del8nt

Ctrl	S T S A R H Q V T T T K Y K S T F E
	AGT ACT TCT GCC CGC CAC CAA <u>GTG</u> ACC ACC ACA AAG TAC AAA TCA ACC TTT GAG

P4-5	S T S A R H H H K V Q I N L *
	AGT ACT TCT GCC CGC CAC CAC AAA GTA CAA ATC AAC CCT TGA

Mex 3 deletion: g.291297delA

Ctrl	S T Q K T S E I T P Q K K A V V Q E E I S Q K A L R
	TCT ACA CAA AAG ACT TCT GAA ATT ACA CCT CAG AAG AAA GCT GTT GTC CAA GAG GAA ATT TCC CAA AAA GCC CTA AGG

P1-3	S T Q R L L K L H L R R K L L S K R K F P K K P *
	TCT ACA CAA AGA CTT CTG AAA TTA CAC CTC AGA AGA AAG CTG TTG TCC AAG AGG AAA TTT CCC AAA AAG CCC TAA

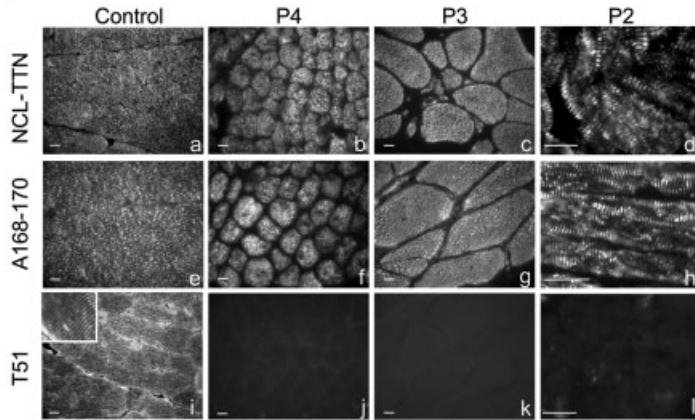
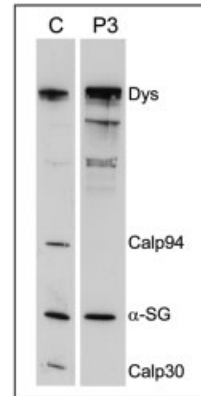
B**C**

Fig 5. (A) Predicted consequences of TTN deletions: reference and mutated mRNA and predicted protein sequences. Both TTN deletions cause frameshifts that generate premature stop codons after changing 8 (Mex1) or 21 (Mex3) amino acid residues. The predicted proteins are truncated 808 and 447 amino acids before their C-terminal end. (B) Presence and sarcomere integration of truncated titin in patient's striated muscles. Titin immunolabeling on striated muscle cryosections from control and patients homozygous for Mex1 (P4) and Mex3 (P2, P3) deletions, using antibodies directed against titin epitopes localized upstream (NCL-TTN [a–d] and A168-170 [e–h]) and downstream (T51 [i–l]) of the mutations. Upstream titin epitopes are present in the patients' skeletal (b, c, f, g) and heart (d, h) muscles; they show a distribution comparable with control muscle (a, e), cross-striated on longitudinal sections (d, h). In contrast, both skeletal muscle (j, k) and myocardium (l) from patients show a complete absence of labeling with T51, suggesting a total loss of C-terminal titin downstream of the m8 domain. Note fiber size variability, including hypertrophic fibers in P3. Longitudinal (d, h, l) and transverse cryosections from control paravertebral muscle (a, e, i), P4 quadriceps (b, f, j), P3 paravertebral (c, g, k), and P2 myocardium (d, h, l). Bar = 20 μm. (C) Multiplex Western blot analysis of calpain in control (C) and P3 skeletal muscle. The blot was labeled with a cocktail of antibodies directed against dystrophin (DYS1; 427kDa), calpain 3 (94 and 30kDa), and α-sarcoglycan (50kDa). In normal muscles, three calpain 3 bands of 94, 60, and 30kDa are detected, the 60 and 30kDa fragments being proteolytic products of the 94kDa protein. Total absence of calpain 3/p94, as well as of the p30 isoform, was observed in the patient homozygous for the Mex3 mutation. Absence of the 60kDa fragment was verified in a separate blot (not shown). Dystrophin and α-sarcoglycan were expressed at the same levels in the patient and the control sample, and served as internal controls. The unlabeled bands correspond to dystrophin degradation products.

muscles. Clinically, skeletal muscle weakness of distinctive distribution was manifest from the first months of life, but remained moderate and relatively stable during the first decade of life. Conversely, heart dysfunction appeared later but progressed quickly, causing death before adulthood. Heart rhythm disturbances led to sudden death in four patients. Although cardiac arrhythmias can be secondarily associated to dilated cardiomyopathy, their frequency and severity in these pa-

tients strongly suggest a primary involvement of the conduction system. Therefore, Holter electrocardiogram must be included from an early age in the follow-up of patients potentially affected by this titinopathy. Successful cardiac transplantation in one case suggests that this is an effective therapy for the cardiac manifestations of this condition.

The histological pattern in young children with TTN deletions is marked by type 1 fiber predomi-

nance, CLNs, and minicore-like lesions, typically found in CMs. Dystrophic lesions suggestive of a CMD and a striking abundance of nonperipheral nuclei appear at later ages. Sequential biopsies of one patient confirmed this age-related evolution of the histological changes. Whether this novel entity should be classified as a CM or a CMD remains to be established; nevertheless, its peculiar clinicomorphological pattern differentiates it from other early-onset muscle disorders. Onset of symptoms in the first year of life is incompatible with the diagnosis of LGMD (contrary to the later onset phenotype of the LGMD2J patients). Marked facial weakness, ptosis, and muscle pseudohypertrophy are not typical of Emery–Dreifuss muscular dystrophy. Mild or moderate creatine kinase increase and normal immunolabeling of sarcolemmal, cytoskeletal, and extracellular matrix proteins distinguish this titinopathy from other muscular dystrophies with dilated cardiomyopathy, including dystroglycanopathies, as well as from myofibrillar myopathies. In contrast, in young children, the differentiation of this new condition from the recessive CM multi-minicore disease¹⁸ is more challenging. Multi-minicore disease is morphologically characterized by minicores that can coexist with type 1 fiber predominance and CLNs, particularly in the multi-minicore disease forms caused by mutations of the *RYR1* gene.^{33–35} Useful distinguishing features can be the absence of heart involvement, central basophilic areas, or severe fibrosis in patients with *RYR1* mutations, as well as the slightly different ultrastructural appearance; in *RYR1*-related cores, Z-line streaming is generally earlier and more evident than M-line disruption.^{18,34}

The pathophysiological consequences of the *TTN* deletions described here can contribute to shed light on the putative functions of M-line titin. It has been suggested that the M-band proteins, including titin, play an important organizational role during myofibrillogenesis.³⁶ Our immunofluorescence data indicate that the truncated titins are incorporated into the sarcomeres; this, together with the normal muscle bulk at birth and the presence of ultrastructurally normal sarcomeres in the homozygous patients, suggests that the titin domains encoded by the last five or three exons are not indispensable for sarcomere assembly and myogenesis in humans.

In contrast, absence of CAPN3 from muscle expressing the homozygous Mex3 deletion indicates disruption of the M-line protein complex and supports the hypothesis that titin stabilizes CAPN3 from autolytic degradation.¹¹ CAPN3 depletion is characteristic of LGMD2A, due to mutations of the *CAPN3* gene (OMIM 114240). It has also been described in LGMD2J, although in these FINmaj patients, as well as in our patients, the second CAPN3 binding site in I-band titin is predicted to be preserved.¹¹ This sug-

gests that the M-line CAPN3-binding site is functionally more relevant in vivo than the I-band site. Absence of CAPN3 could play a role in the skeletal muscle loss observed in our patients; however, CAPN3 is not expressed in mature heart muscle.¹¹ Therefore, defective titin-CAPN3 interaction, CAPN3 depletion, or both cannot explain completely the disease mechanism in this novel titinopathy.

It cannot be excluded that large M-band titin deletions lead to loss of interaction with other currently uncharacterized ligands. Yet, a relevant mechanism in this disease could be loss of the mechanical stability of the sarcomeres. One of the main proposed functions of titin is to keep the contractile elements of the sarcomere in place.³⁷ The sarcomere disarray observed in our patients suggests that the M-line titin segments downstream of the kinase domain contribute significantly to maintenance of sarcomeric integrity. Previous human *TTN* mutations do not cause major sarcomere disruptions. Interestingly, the sarcomere disarray and CLNs in our patients resemble those described in a mouse model selectively deleted of *TTN* exons Mex1 and Mex2.³⁸ This so-called M-line-deficient mouse shows loss of the kinase domain and the known binding sites for MURF1, DRAL/FHL2, and myomesin, with normal expression of exons Mex3 to Mex6.^{14,38,39} In contrast, mutations in our patients localize more than 1,000 residues downstream the kinase domain, respect the above-mentioned binding sites, and lead to deletion of the last three or five exons. Thus, defects in consecutive portions of M-line titin have similar histopathological consequences. This suggests that, contrary to previous hypothesis,³⁸ the sarcomere disassembly observed in the mice might be unrelated with titin kinase, myomesin, or MURF1. According to our results, it is tempting to speculate that any significant titin disruption affecting the region of C-terminal antiparallel overlap between two opposite titin molecules¹⁹ could lead to reduced M-line stability and ultimately to sarcomere disassembly under stretch or active mechanical load. Heart muscle being constantly submitted to these mechanical circumstances, this mechanism could contribute to explaining the relatively late but fatal cardiac phenotype in our patients.

An unexpected finding in this study was the absence of any clinical or radiological phenotype in the heterozygous carriers of the Mex1 and Mex3 deletions, including those currently close to the seventh decade. The two previously reported mutations causing truncated titins are localized in the first third of the protein,^{8,9} which might explain why they manifest (as heart failure) in the heterozygous state. More difficult to explain is that heterozygous amino acid changes caused by Mex6 mutations lead to TMD, whereas large deletions including this exon remain phenotypically silent in the heterozygous carriers. Interestingly,

biallelic deletion of the entire M-line titin coding region in mouse embryonic stem cells results in failure to differentiate into cardiomyocytes, whereas deletion of one allele does not affect differentiation.⁴⁰ These recent data are consistent with the absence of phenotype in our heterozygous carriers, which could also be explained by degradation of the mutated messenger RNA through nonsense-mediated decay or by a dominant-negative effect of the previously reported *Mex6* changes. Further studies are in progress to substantiate these hypotheses.

In conclusion, our results demonstrate that homozygous truncations of M-line titin preserving the kinase domain are compatible with life but cause a severe and distinct disorder, which expands the nosological spectrum of early-onset myopathies. We propose that recessive titin defects should be looked for in idiopathic pediatric cardiomyopathy, for which a minority of causes is known. Titin defects should also be considered in patients whose skeletal muscle shows minicore-like lesions associated with numerous CLNs and/or *CAPN3* deficiency without *CAPN3* mutations. Absence of *CAPN3* suggests that disruption of the M-line protein complex is a pathogenic mechanism in this new entity. Also, this work stresses the functional relevance of the M-line titin segments downstream the kinase domain, suggesting that, although they are dispensable for muscle or heart formation, they play a role in maintaining sarcomere integrity in contracting muscles. Further studies are in progress to determine precise pathophysiological consequences of 3' M-line titin deletions at the mRNA, protein, and cellular levels.

The following databases were used in the preparation of this article: www.ensembl.org; <http://www.ncbi.nlm.nih.gov>; <http://genecards.weizmann.ac.il/geneloc>; OMIM: <http://www.ncbi.nlm.nih.gov/entrez/query.fcgi?db=OMIM>. Accession numbers are as follows: titin genomic sequence—GeneBank, AJ277892; titin isoform N2A mRNA sequence—NM_133378.2.

This work was supported by the Institut National de la Santé et de la Recherche Médicale (INSERM), the Association Française contre les Myopathies, the British Heart Foundation (M.G.), the European Union MYORES network (M.G.), the Medical Research Council of Great Britain (G0600251, M.G.), the INSERM (Conseil Régional d'Ile-de France grant, R03069DS-RSE03004DSA, V.C.), and an Avenir Career Development Award (R03119DS-RAE03002DSA, A.F.).

We thank the patients and their families for their participation in this study. The Centre National de Génotypage (France) provided technical assistance for genome screen; Dr P. Richard helped with muscle DNA extraction. Prof J.-P. Leroy, Dr N. Romero, and E. Lacene contributed to the morphological and ultrastructural studies; Dr Furnet helped us to retrieve postmortem muscle samples. We thank Dr Sir K. Hashim for his contribution to the clinical follow-up of the Sudanese family, Dr C. Lafuente for useful discussion of the cardiac arrhythmias, and Dr N. Clarke for critical reading of the manuscript.

References

- Fardeau M, Tomé F. Congenital myopathies. In: Engel AG, Franzini-Armstrong C, eds. *Myology*. 2nd ed. New York: McGraw-Hill, 1994:1487–1532.
- Muntoni F, Voit T. The congenital muscular dystrophies in 2004: a century of exciting progress. *Neuromuscul Disord* 2004;14:635–649.
- Jungbluth H, Sewry CA, Muntoni F. What's new in neuromuscular disorders? The congenital myopathies. *Eur J Paediatr Neurol* 2003;7:23–30.
- Bitoun M, Maugrenre S, Jeannet PY, et al. Mutations in dynamin 2 cause dominant centronuclear myopathy. *Nat Genet* 2005;37:1207–1209.
- Labeit S, Kolmerer B. Titins: giant proteins in charge of muscle ultrastructure and elasticity. *Science* 1995;270:293–296.
- Satoh M, Takahashi M, Sakamoto T, et al. Structural analysis of the titin gene in hypertrophic cardiomyopathy: identification of a novel disease gene. *Biochem Biophys Res Commun* 1999;262:411–417.
- Matsumoto Y, Hayashi T, Inagaki N, et al. Functional analysis of titin/connectin N2-B mutations found in cardiomyopathy. *J Muscle Res Cell Motil* 2005;26(6–8):367–374.
- Gerull B, Gramlich M, Atherton J, et al. Mutations of TTN, encoding the giant muscle filament titin, cause familial dilated cardiomyopathy. *Nat Genet* 2002;30:201–204.
- Itoh-Satoh M, Hayashi T, Nishi H, et al. Titin mutations as the molecular basis for dilated cardiomyopathy. *Biochem Biophys Res Commun* 2002;291:385–393.
- Lange S, Xiang F, Yakovenko A, et al. The kinase domain of titin controls muscle gene expression and protein turnover. *Science* 2005;308:1599–1603.
- Hackman P, Vihola A, Haravuori H, et al. Tibial muscular dystrophy is a titinopathy caused by mutations in TTN, the gene encoding the giant skeletal-muscle protein titin. *Am J Hum Genet* 2002;71:492–500.
- Van den Bergh PY, Bouquiaux O, Verellen C, et al. Tibial muscular dystrophy in a Belgian family. *Ann Neurol* 2003;54:248–251.
- Udd B, Vihola A, Sarparanta J, et al. Titinopathies and extension of the M-line mutation phenotype beyond distal myopathy and LGMD2J. *Neurology* 2005;64:636–642.
- Gotthardt M, Hammer RE, Hubner N, et al. Conditional expression of mutant M-line titins results in cardiomyopathy with altered sarcomere structure. *J Biol Chem* 2003;278:6059–6065.
- van der Ven PF, Bartsch JW, Gautel M, et al. A functional knock-out of titin results in defective myofibril assembly. *J Cell Sci* 2000;113:1405–1414.
- Salih MA, Al Rayess M, Cutshaw S, et al. A novel form of familial congenital muscular dystrophy in two adolescents. *Neuropediatrics* 1998;29:289–293.
- Subahi SA. Distinguishing cardiac features of a novel form of congenital muscular dystrophy (Salih cmd). *Pediatr Cardiol* 2001;22:297–301.
- Ferreiro A, Estournet B, Chateau D, et al. Multi-minicore disease—searching for boundaries: phenotype analysis of 38 cases. *Ann Neurol* 2000;48:745–757.
- Obermann WM, Gautel M, Steiner F, et al. The structure of the sarcomeric M band: localization of defined domains of myomesin, M-protein, and the 250-kD carboxy-terminal region of titin by immunoelectron microscopy. *J Cell Biol* 1996;134:1441–1453.

20. Ferreiro A, Quijano-Roy S, Pichereau C, et al. Mutations of the selenoprotein N gene, which is implicated in rigid spine muscular dystrophy, cause the classical phenotype of multiminicore disease: reassessing the nosology of early-onset myopathies. *Am J Hum Genet* 2002;71:739–749.
21. Brockington M, Blake DJ, Prandini P, et al. Mutations in the fukutin-related protein gene (FKRP) cause a form of congenital muscular dystrophy with secondary laminin alpha2 deficiency and abnormal glycosylation of alpha-dystroglycan. *Am J Hum Genet* 2001;69:1198–1209.
22. Bonne G, Di Barletta MR, Varnous S, et al. Mutations in the gene encoding lamin A/C cause autosomal dominant Emery-Dreifuss muscular dystrophy. *Nat Genet* 1999;21:285–288.
23. Fananapazir L, Dalakas MC, Cyran F, et al. Missense mutations in the beta-myosin heavy-chain gene cause central core disease in hypertrophic cardiomyopathy. *Proc Natl Acad Sci U S A* 1993;90:3993–3997.
24. Lindner TH, Hoffmann K. easyLINKAGE: a PERL script for easy and automated two-/multi-point linkage analyses. *Bioinformatics* 2005;21:405–407.
25. Marchand S, Hajdari P, Hackman P, et al. Touch-down method for high-performance sequencing of polymerase chain reaction products. *Anal Biochem* 2003;315:270–272.
26. Anderson LV, Davison K, Moss JA, et al. Characterization of monoclonal antibodies to calpain 3 and protein expression in muscle from patients with limb-girdle muscular dystrophy type 2A. *Am J Pathol* 1998;153:1169–1179.
27. Kolmerer B, Olivier N, Witt CC, et al. Genomic organization of M line titin and its tissue-specific expression in two distinct isoforms. *J Mol Biol* 1996;256:556–563.
28. Gregorio CC, Granzier H, Sorimachi H, Labeit S. Muscle assembly: a titanic achievement? *Curr Opin Cell Biol* 1999;11:18–25.
29. Miller G, Musa H, Gautel M, Peckham M. A targeted deletion of the C-terminal end of titin, including the titin kinase domain, impairs myofibrillogenesis. *J Cell Sci* 2003;116:4811–4819.
30. Labeit S, Gautel M, Lakey A, Trinick J. Towards a molecular understanding of titin. *EMBO J* 1992;11:1711–1716.
31. Improta S, Krueger JK, Gautel M, et al. The assembly of immunoglobulin-like modules in titin: implications for muscle elasticity. *J Mol Biol* 1998;284:761–777.
32. Linke WA, Kulke M, Li H, et al. PEVK domain of titin: an entropic spring with actin-binding properties. *J Struct Biol* 2002;137:194–205.
33. Ferreiro A, Monnier N, Romero NB, et al. A recessive form of central core disease, transiently presenting as multi-minicore disease, is associated with a homozygous mutation in the ryanodine receptor type 1 gene. *Ann Neurol* 2002;51:750–759.
34. Sewry CA, Muller C, Davis M, et al. The spectrum of pathology in central core disease. *Neuromuscul Disord* 2002;12:930–938.
35. Monnier N, Ferreiro A, Marty I, et al. A homozygous splicing mutation causing a depletion of skeletal muscle RYR1 is associated with multi-minicore disease congenital myopathy with ophthalmoplegia. *Hum Mol Genet* 2003;12:1171–1178.
36. Wang SM, Lo MC, Shang C, et al. Role of M-line proteins in sarcomeric titin assembly during cardiac myofibrillogenesis. *J Cell Biochem* 1998;71:82–95.
37. Horowitz R, Maruyama K, Podolsky RJ. Elastic behavior of connectin filaments during thick filament movement in activated skeletal muscle. *J Cell Biol* 1989;109:2169–2176.
38. Peng J, Radatz K, Labeit S, et al. Muscle atrophy in Titin M-line deficient mice. *J Muscle Res Cell Motil* 2005;26:381–388.
39. Weinert S, Bergmann N, Luo X, et al. M line-deficient titin causes cardiac lethality through impaired maturation of the sarcomere. *J Cell Biol* 2006;173:559–570.
40. Musa H, Meek S, Gautel M, et al. Targeted homozygous deletion of M-band titin in cardiomyocytes prevents sarcomere formation. *J Cell Sci* 2006;119:4322–4331.